# Peroxygenase and Oxidase Activities of Dehaloperoxidase-Hemoglobin from *Amphitrite ornata*

David A. Barrios, Jennifer D'Antonio, Nikolette L. McCombs, Jing Zhao, Stefan Franzen, Andreas C. Schmidt, Leslie A. Sombers, and Reza A. Ghiladi*

Department of Chemistry, North Carolina State University, Raleigh, North Carolina 27695-8204, United States

S *Supporting Information*

ABSTRACT: The marine globin dehaloperoxidase-hemoglobin (DHP) from *Amphitrite ornata* was found to catalyze the H_2O_2-dependent oxidation of monohaloindoles, a previously unknown class of substrate for DHP. Using 5-Br-indole as a representative substrate, the major monooxygenated products were found to be 5-Br-2-oxindole and 5-Br-3-oxindolenine. Isotope labeling studies confirmed that the oxygen atom incorporated was derived exclusively from H_2O_2, indicative of a previously unreported peroxygenase activity for DHP. Peroxygenase activity could be initiated from either the ferric or oxyferrous states with equivalent substrate conversion and product distribution. It was found that 5-Br-3-oxindole, a precursor of the product 5-Br-3-oxindolenine, readily reduced the ferric enzyme to the oxyferrous state, demonstrating an unusual product-driven reduction of the enzyme. As such, DHP returns to the globin-active oxyferrous form after peroxygenase activity ceases. Reactivity with 5-Br-3-oxindole in the absence of H_2O_2 also yielded 5,5′-Br_2-indigo above the expected reaction stoichiometry under aerobic conditions, and O_2-concentration studies demonstrated dioxygen consumption. Nonenzymatic and anaerobic controls both confirmed the requirements for DHP and molecular oxygen in the catalytic generation of 5,5′-Br_2-indigo, and together suggest a newly identified oxidase activity for DHP.
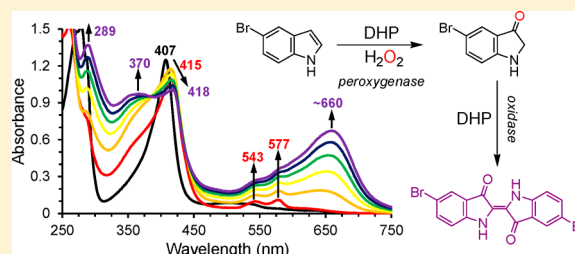
INTRODUCTION

A longstanding question in catalysis is how structure plays a role in influencing chemical reactivity. This is readily apparent in heme proteins where O_2-binding, oxygenase, oxidase, peroxygenase, and electron-transfer reactions all occur at active sites that often contain a surprising number of similarities, both structural and, by consequence, mechanistic. For example, the reactive heme species known as Compound I contains an Fe(IV)-oxo (ferryl) and porphyrin π-cation radical and has been implicated in the mechanisms of cytochrome *c* oxidase,[1] cytochrome P450 monooxygenase,[2] human indoleamine 2,3-dioxygenase,[3] the fungal peroxygenase *Aae*APO,[4] horseradish peroxidase,[5] and prostaglandin endoperoxidase synthase (cyclo-oxygenase)[6] and has even been shown to form in myoglobin.[7] Despite the common intermediate, the chemical reactivity of each of the aforementioned systems remains exquisitely controlled by the protein structure[6] to ensure maximum intended function with a minimum of unintended cross reactivity. How nature achieves this control for the selectivity of function continues to be of interest, yet remains a significant challenge to fully understand.

Our chosen platform for the elaboration of the structural features and other determinants that impart specific discrete functions to heme proteins is the enzyme dehaloperoxidase (DHP), the coelomic hemoglobin from the marine worm *Amphitrite ornata*.[8-10] DHP has also been shown to possess a biologically relevant peroxidase activity that is believed to have arisen from the evolutionary pressure to overcome high levels
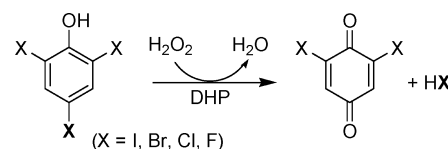
Figure 1. Reaction of DHP with trihalogenated phenols and hydrogen peroxide yields quinone products.

of volatile brominated secondary metabolites that are secreted as repellents by other infaunal marine organisms that co-inhabit the benthic ecosystems within which *A. ornata* is found.[10,11] The oxidative dehalogenation of 2,4,6-trihalophenol yielding 2,6-dihaloquinone (Figure 1) has been investigated for both known isoenzymes of DHP (A and B).[12-23] The DHP peroxidase cycle can be initiated from both the ferric and ferrous (or oxyferrous) oxidation states.[17,22] When starting from the ferric state, DHP appears to function via a Poulos-Kraut type mechanism[24] in which H_2O_2 reacts with a ferric heme to form DHP Compound I,[18,21] the iron(IV)-oxo porphyrin π-cation radical species that is formally two electrons oxidized relative to the ferric resting state. Compound I rapidly converts in DHP to an iron(IV)-oxo heme center with an amino acid radical that has been termed Compound ES by analogy with cytochrome *c* peroxidase.[13-15,18,21] These peroxide-activated forms of DHP return to the ferric resting

state upon oxidation of substrate in what is likely two consecutive one-electron steps.[20] Thus, although the activated heme of dehaloperoxidase can theoretically support a direct oxygen atom transfer, no peroxygenase activity has been reported for DHP.

In an effort to identify whether DHP is capable of oxygen atom transfer chemistry, we have expanded the substrate scope of our reactivity studies to include other halometabolites that are native to the marine environment of *A. ornata*. Given the diversity of naturally occurring organobromine compounds found in benthic ecosystems (e.g., mono-, di-, and tribromophenols, mono- and dibromovinylphenols, bromopyrroles),[25−27] we have limited the current study to brominated indoles, as these have been isolated from several species of the Hemichordata phylum that cohabitate with *A. ornata* in coastal estuaries,[28,29] and may represent another family of chemical deterrents evolutionarily targeted by *A. ornata* and DHP. Furthermore, similar marine-related indoles and their derivatives continue to gain interest as antimicrobial and/or anticancer agents (e.g., meridianins, fascaplysin)[30−33] and are emerging as a new class of compounds for further study.

Herein, we have investigated the ability for DHP to catalyze the oxidation of haloindoles in the presence of H_2O_2. The reaction products were identified in the presence and absence of labeled peroxide, and the results provide unequivocal evidence that DHP is capable of a previously unreported peroxygenase activity that is similar to that observed for the peroxide shunt pathways of both P450 monooxygenase and indoleamine 2,3-dioxygenase.[2,34−36] The peroxygenase activity was observed to be initiated from either the ferric or oxyferrous states, with the enzyme returning to the oxyferrous state upon completion of its activity due to an unusual product-driven oxidase reaction that ultimately forms indigo derivatives as products. The fact that the peroxygenase activity is initiated from, and returns to, the oxyferrous state is likely related to the primary function of DHP of serving as an oxygen transport protein, yet also highlights the plasticity of the DHP active site for supporting multiple enzymatic functions.

RESULTS

DHP-Catalyzed Haloindole Reactivity with H_2O_2. The hydrogen peroxide-dependent oxidation of haloindoles as catalyzed by ferric WT DHP B at pH 7 was monitored by HPLC. Reactions were initiated upon addition of 500 μM H_2O_2 to a solution containing 10 μM enzyme and 500 μM indole, incubated at 25 °C for 5 min and then quenched with catalase. Reactivity was greatest with 5-Br-indole (Table 1), but overall a <1.5-fold difference in reactivity was observed as the position of the bromine substituent was varied (5-Br ≈ 7-Br > 4-Br > 6-Br). Indole itself also showed reactivity, albeit 2-fold lower than 5-Br-indole. Reactivity across the halogen series of 5-X-indoles was also <2-fold varied and was observed as follows: Br > Cl ≈ I > F ≈ H. These results suggest that neither the sterics nor the electronics of the substrate play a significant role in its conversion. No reactivity was observed when either DHP (non-enzymatic control) or peroxide (non-oxidant control) were excluded from the reaction.

The reactivity with 5-Br-indole was virtually identical for oxyferrous DHP B compared to the ferric enzyme, indicating that the reaction can be initiated from either the globin active ($Fe^{II}−O_2$) or peroxidase-active (Fe^{III}) states, a result that has been observed previously for TCP oxidation.[17,22] The mutant DHP B(Y28F/Y38F), which forms Compound I rather than

Table 1. Enzyme-Catalyzed Reactivity of Haloindoles[a]

enzyme	conversion (%)
Substrate Variation	
DHP B Ferric	
+ indole	24.1 (±2.3)
+ 4-Br-indole	41.1 (±2.0)
+ 5-Br-indole	48.1 (±2.3)
+ 6-Br-indole	34.4 (±0.6)
+ 7-Br-indole	46.1 (±1.7)
+ 5-F-indole	26.0 (±1.3)
+ 5-Cl-indole	37.5 (±1.6)
+ 5-I-indole	34.0 (±2.0)
+ tryptophan	n.d.[b]
Enzyme Variation	
DHP B Oxyferrous	
+ 5-Br-indole	44.9 (±4.8)
DHP B (Y28/38F) Ferric	
+ 5-Br-indole	62.2 (±2.5)
DHP A Ferric	
+ 4-Br-indole	15.7 (±0.7)
+ 5-Br-indole	20.3 (±1.7)
HRP	
+ 5-Br-indole	n.d.
hhMb	
+ 5-Br-indole	n.d.
Mechanistic Probes	
DHP B Ferric	
anaerobic + 4-Br-indole	40.1 (±0.9)
anaerobic + 5-Br-indole	53.3 (±0.3)
DHP B Ferric (+ 5-Br-indole)	
+ 500 μM mannitol	46.2 (±1.6)
+ 500 mM formate	45.8 (±1.1)
+ SOD[c]	46.1 (±0.7)
+ 10% DMSO	45.0 (±4.4)
+ 500 μM 4-BP	23.2 (±5.1)
pH Effects	
DHP B Ferric (+ 5-Br-indole)	
pH 5	63.4 (±0.1)
pH 6	54.7 (±1.9)
pH 7	48.1 (±2.2)
pH 8	34.4 (±2.4)

[a]Reaction conditions: [haloindole] = [H_2O_2] = 500 μM, [enzyme] = 10 μM, 5% MeOH in 100 mM KP$_i$ buffer at pH 7 (unless indicated), 25 °C, 5 min. [b]n.d. = none detected. [c]SOD = ~2 U/μL.

the Compound ES species observed in WT DHP B,[18] was only 1.3-fold more reactive with 5-Br-indole, which is approximately in line with the ratio of the catalytic efficiencies (k_{cat}/K_m) of these two enzymes for TCP oxidation (~1.6).[18] WT DHP B was also found to be ~2.4-fold more reactive than WT DHP A, which is nearly identical to the ratio observed (2.6-fold) for TCP oxidation.[14] In the presence of 500 μM 4-bromophenol, a known inhibitor of TCP oxidation,[37] a 2-fold attenuation in reactivity was observed for 5-Br-indole.

Reactions performed in the presence of radical scavengers (DMSO, sodium formate, D-mannitol) and superoxide dismutase (SOD) all showed nearly equivalent 5-Br-indole reactivity when compared to the reaction run in their absence. No changes in product distribution were observed by HPLC (*vide infra*) in the presence of these radical scavengers. Reactions performed anaerobically under N_2 showed no decrease in reactivity, consistent with previous studies of WT
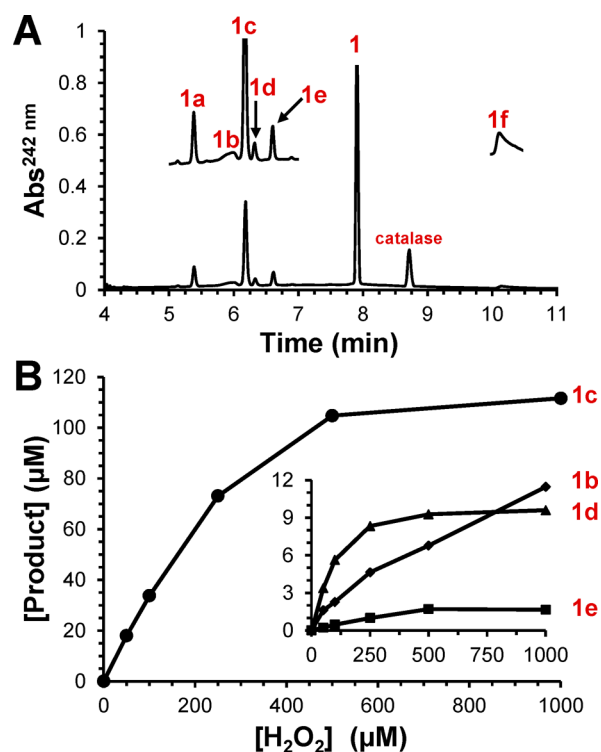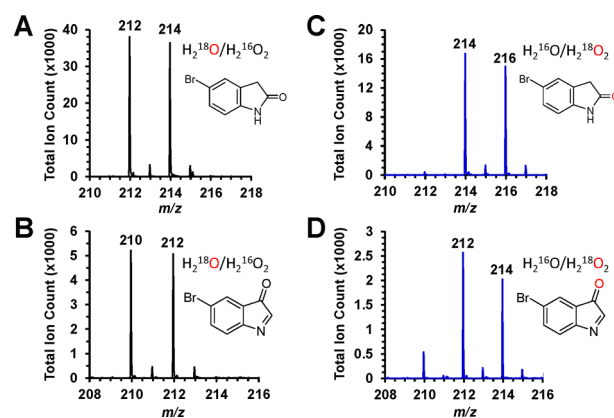
Figure 2. (A) HPLC chromatogram of the reaction of 5-Br-indole (500 μM) with DHP B (10 μM) in the presence of H_2O_2 (500 μM) at 25 °C (5% MeOH in 100 mM KP_i, pH 7). The reaction was quenched upon addition of catalase and subjected to HPLC analysis as described in the text. (B) Product distribution for the reaction described in panel A under variable [H_2O_2].

Figure 3. ESI-MS total ion chromatograms obtained for the reaction products 5-Br-2-oxindole (A: $H_2^{18}O$, $H_2^{16}O_2$; C: $H_2^{16}O$, $H_2^{18}O_2$) and 5-Br-3-oxindolenine (B: $H_2^{18}O$, $H_2^{16}O_2$; D: $H_2^{16}O$, $H_2^{18}O_2$). Reaction conditions: [haloindole] = [H_2O_2] = 500 μM, [enzyme] = 10 μM, 5% MeOH in 100 mM KP_i (pH 7), 25 °C.

DHP B and TCP that demonstrated an O_2-independent reaction pathway.[14,17] Finally, studies performed with horse-radish peroxidase (HRP) or horse heart myoglobin (Mb), the respective archetypes of the peroxidase and globin super-families, showed no reactivity with 5-Br-indole substrate.

Identification of Reaction Products by HPLC. A representative HPLC trace at 242 nm is shown in Figure 2A for studies performed with 5-Br-indole (**1**). Products were identified by their characteristic retention time and electronic absorption spectrum as compared to authentic samples (Figure S1), by similarity to those of their respective unsubstituted analogue when the halogenated versions were not commercially available,[36] and/or by mass spectrometry (*vide infra*). Two major products were identified: 5-Br-2-oxindole (**1c**, 44%) and 5-Br-3-oxindolenine (**1a**, ~47% as determined from mass balance). Minor products were also noted: the doubly oxygenated products 5-Br-2,3-dioxindole (**1b**, 2.9%) and 5-Br-3-hydroxy-2-oxindole (**1d**, 3.7%), the pyrrole ring-opened product *N*-(4-Br-2-formylphenyl)formamide (**1e**, 0.6%), and the indigo derivative (*E*)-5,5′-dibromo-[2,2′-biindolinylidene]-3,3′-dione (**1f**, ~2%).

Control reactions with 5-Br-2-oxindole as the substrate under the same reaction conditions showed no further chemistry, suggesting no secondary oxidation products were derived from this species. 5-Br-3-oxindole was not observed directly, with its oxidation likely giving rise to the observed 5-Br-3-oxindolenine and/or secondary oxidation products (*vide infra*). A similar product distribution was observed for studies performed with indole (Figure S2A).

Product Distribution as a Function of H_2O_2 Concentration. The distribution of products for studies performed with 5-Br-indole (500 μM) was monitored as a function of H_2O_2 concentration (Figure 2B). With one exception, the formation of all products was linear as a function of peroxide concentration up to 100 μM ([indole] > [H_2O_2]), yet reached a plateau above 500 μM ([indole] < [H_2O_2]). The ratio of the products formed was nearly constant regardless of the H_2O_2 concentration employed (Table S1). The lack of further product formation under conditions of excess peroxide is in line with previous observations that DHP enters a peroxidase-attenuated state, Compound RH,[8,13−15,18] under conditions of low [substrate]. As the exception, 5-Br-2,3-dioxindole formed linearly throughout the tested H_2O_2 concentration range, suggesting a non-enzymatic process under conditions of excess peroxide. A similar H_2O_2 concentration-dependent product distribution profile was observed for studies performed with indole (Figure S2B, Table S1).

Isotopically Labeled Oxygen Studies. As the observed reactivity was O_2-independent (anaerobic study, Table 1), studies employing labeled $H_2^{18}O_2$ and $H_2^{18}O$ (90% and 98% oxygen atom enriched, respectively) were performed with 5-Br-indole and subsequently analyzed by LC-MS to determine the source of the oxygen atom incorporation. The background-subtracted total ion chromatograms (TICs) are shown in Figure 3. The isotopic distributions for the major products observed, 5-Br-2-oxindole and 5-Br-3-oxindolenine, were determined using previously established methods.[36,38] Products were identified by the respective *m/z* of the (M + H)$^+$ ion and retention time as compared to available standards. In the absence of an ^{18}O source, both 5-Br-2-oxindole (*m/z*: 212, 99.2%; 214:100%) and 5-Br-3-oxindolenine (*m/z*: 210, 96.9%; 212:100%) exhibited masses with the expected ca. 1:1 isotopic distribution for bromine (Table S2). In the presence of $H_2^{18}O$ and unlabeled H_2O_2, neither product exhibited an increase in mass: 5-Br-2-oxindole (*m/z*: 212, 99.8%; 214, 100%; Figure 3A) and 5-Br-3-oxindolenine (*m/z*: 210, 100%; 212, 99.4%; Figure 3B). The parent ions also exhibited their expected ~1:1 relative abundance, and thus solvent water was ruled out as the source of the oxygen atom incorporated. These same experiments employing $H_2^{18}O_2$ and unlabeled $H_2^{18}O$ showed a clear increase to higher mass for both products by 2 Da: 5-Br-2-oxindole (*m/z*: 212, 6.1%; 214, 100%; 216, 75.8%; Figure

3C) and 5-Br-3-oxindolenine (m/z: 210, 4.7%; 212, 100%; 214, 89.5; Figure 3D). The results showed a 97+% ^{18}O enrichment (normalized), providing unequivocal evidence that the oxygen atom was derived from H_2O_2. The minor dioxygenated products were of too low concentration to be observed, and their origins were not pursued further at the time.

In studies with indole (m/z: 134, 100%; Table S2), the oxygen incorporated into the respective 2-oxindole product was derived from $H_2^{18}O_2$ (m/z: 134, 10.1%; 136, 100%; ~100% normalized ^{18}O enrichment) and not from $H_2^{18}O$ (m/z: 134, 100%; 136, 0.8%), consistent with the results from above for 5-Br-indole. However, the results for the 3-oxindolenine product showed some scrambling of the label. Experiments run in $H_2^{18}O_2$ and unlabeled water exhibited 51.8% ^{18}O enrichment (normalized), whereas those run with $H_2^{18}O$ and unlabeled water yielded minimal label incorporation (5.5%). Reactions performed with both $H_2^{18}O_2$ and $H_2^{18}O$ showed 60.1% ^{18}O enrichment. The reasons for why the ^{18}O enrichment for 5-Br-3-oxindolenine was nearly quantitative versus ~50% for 3-oxindolenine for experiments performed under identical reaction conditions and work-up times remain unclear.

Resonance Raman Studies. Resonance Raman spectra were collected of ferric WT DHP B in the presence of 10 equiv haloindoles in 10% MeOH/100 mM KP_i (v/v) at pH 7. Compared to aqueous buffer, there is a significant increase in the 6-coordinated high spin (6cHS) heme Fe in 10% MeOH buffer solution. The red spectrum in Figure 4A shows that the heme Fe is nearly 100% 6cHS with H_2O bound to the heme Fe, while in aqueous solution there is a mixture of 5-coordinated high spin (5cHS) and 6cHS metaquo heme as observed in previous work.[37] Presumably, this arises from a destabilization of the distal histidine (His[55]) in the solvent exposed (or "open") conformation in the 10% MeOH buffer solution. The fact that His55 appears to favor the internal or "closed" conformation means that the contrast shown in Figure 4A
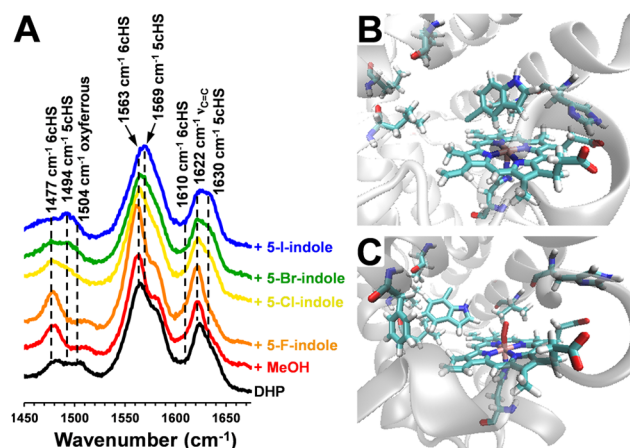
Figure 4. (A) Resonance Raman spectra of 5-X-indole (500 μM; X = F, Cl, Br, I) complexes of DHP B (50 μM) in 10% MeOH/100 mM KP_i (v/v) at pH 7. (B) Geometry optimized structure for 5-Br-indole. The 5-bromoindole model was obtained by replacement of 4-bromophenol in the PDB 3LB2 structure.[37] In this model, the bromine atom is located in the Xe binding site[39] as observed in the 4-bromophenol structure. (C) Geometry optimized structure for 7-Br-indole. The native substrate 2,4,6-tribromophenol (2,4,6-TBP) in the structure PDB 4HF6[40] was substituted with 7-bromoindole. Since diatomic O_2 was observed bound to the heme Fe in that structure, the bound O_2 was preserved in this model.

between free DHP (no added indole substrate) and the various indole substrates is larger than observed in previous work in aqueous solution.

Neither indole nor bromoindoles (4-, 6-, or 7-Br) caused a significant perturbation in the high-frequency region (Figure S3) when compared to the DHP only sample. However, 5-Br-indole exhibited an increase in the core size marker bands (ν_3 = 1494 cm^{-1}; ν_2 = 1569 cm^{-1}; ν_{10} = 1630 cm^{-1}) attributed to 5cHS heme and a decrease in those for 6cHS heme (ν_3 = 1477 cm^{-1}; ν_2 = 1563 cm^{-1}). As such, the spectra for the 5-substituted halogen series were investigated (Figure 4A). A decrease in the modes assigned to the 6cHS heme population and an increase in those for 5cHS heme that follows the halogen series (I > Br > Cl > F) was observed.

Similar observations for halophenols have been noted,[37,41] where their binding to DHP has been shown to perturb the relative population of 5cHS vs 6cHS high spin ferric heme. Specifically, 4-halophenols, known inhibitors of DHP,[37] bind in the distal pocket, displacing the distal histidine (His[55]) into an "open" or solvent exposed confirmation. This limits the availability of His[55] to stabilize an iron-bound water ligand through hydrogen bonding, thus shifting the relative population from primarily 6cHS heme to predominantly 5cHS heme, with the magnitude of the shift correlating with the size of the halogen atom.[37,41] We envision a similar process occurring here with 5-haloindoles, where their binding to the active site of DHP results in the displacement of the distal histidine, loss of the water ligand, and increase in the 5cHS heme population. As shown in Figure 4B, the geometry optimized structure for 5-Br-indole binding to DHP B, where the indole occupies the space right above the heme iron (i.e., the monohalophenol inhibitor site), is consistent with this hypothesis. By contrast, the geometry optimized structure shown in Figure 4C shows that the DHP B active site can accommodate a 6cHS heme when 7-Br-indole is bound off of the α-edge of the heme (i.e., the trihalophenol substrate site). These calculations show that 5-bromo- and 7-bromoindole fit in the inhibitor and substrate binding sites, respectively, consistent with the results from the resonance Raman spectroscopic studies.

5-Haloindole Binding Studies. The electronic absorption spectra of ferric DHP B in the presence of 50 equiv 5-Br-indole [402 (Soret), 508, 540 (sh), 585, 635 nm] and alone [407 (Soret), 507, 540 (sh), 635 nm] were recorded in 100 mM KP_i (pH 7) containing 10% MeOH (v/v) (Figure S4). Using the observed hypochromicity and hypsochromic shift of the Soret band upon 5-Br-indole binding, optical difference spectra were recorded per literature protocol as a function of substrate concentration (2.5–100 equiv; Figure S5).[42] Analysis by nonlinear regression provided a calculated A_{max} of 0.51, which was in turn used to calculate α for the average ΔA for each [5-Br-indole]. A second nonlinear regression plot provided an apparent dissociation constant (K_d) of 150 ± 10 μM. Similarly, the K_d values were experimentally determined for the other 5-substituted halogens (5-Cl-indole: 317 ± 23 μM; 5-I-indole: 62 ± 10 μM). No significant changes in the optical difference spectra were observed for 5-F-indole even at the highest concentrations tested, and as such its binding affinity was suggested to be weaker than 5-Cl-indole. Overall, a trend in K_d was observed of increasing binding affinity as the size of the halogen atom was increased: F < Cl < Br < I. For the latter three indoles whose K_d values were experimentally determined, all exhibited higher affinity for DHP than 4-bromophenol (K_d ~ 1.2 mM),[37] a known inhibitor of the enzyme.

Stopped-Flow Studies with Ferric DHP B. Double-mixing stopped-flow UV−vis spectroscopic methods were used to investigate the reaction of 5-Br-indole with H_2O_2-activated DHP, preformed either as Compound ES (WT DHP) or Compound I [DHP B(Y28F/Y38F)]. Ferric WT DHP B (10 μM) was reacted with 10 mol equiv of H_2O_2 at pH 7, incubated for 350 ms to allow for the maximum accumulation of Compound ES,[14] and subsequently mixed with 10, 25, or 50 equiv of 5-Br-indole. When reacted with 10 equiv substrate (Figure 5), the preformed Compound ES [UV−vis: 418 (Soret), 545, 583 nm] was rapidly reduced [$k_{obs} = (2.54 \pm 0.05) \times 10^5$ M^{-1} s^{-1}] to a species whose spectral features we attribute to substrate- (or possibly product-) bound ferric DHP B [406 (Soret), 508, 540 (sh), and 633 nm] (see Figure S4 for comparison). For substrate concentrations ≥25 equiv 5-Br-indole, no Compound ES was observed. Rather, it was rapidly reduced within the mixing time of the stopped-flow apparatus (<2.5 ms), and only the ferric enzyme was observed initially. For all substrate concentrations examined, the ferric enzyme was found to convert to a species [418 (Soret), 544, 577, 590 (sh) nm] that is similar, but not identical, to Compound ES/II (these two species being indistinguishable by optical spectroscopy for DHP[17,18]) and is described as indole-derived ferryl DHP (vide infra). This was likely attributable to the reaction of the initially produced ferric enzyme with the excess H_2O_2 employed in this study. At longer observation times, a new species [414 (Soret), 540, 577 nm; $k_{obs} = (1.39 \pm 0.08) \times 10^{-2}$ s^{-1}] was noted whose spectral features matched those of a mixture of oxyferrous DHP B and the ferric enzyme.[14,17] Under these conditions of excess substrate, Compound RH, the stable form of DHP that forms from H_2O_2 activation in the absence of substrate, was not observed.

The 5-Br-indole reactivity studies performed with preformed Compound I using DHP B(Y28F/Y38F) were qualitatively the same as those reported above for preformed Compound ES using WT DHP B (Figure S6) with the exception that no activated enzyme (i.e., preformed Compound I [406 (Soret), 528, and 645 nm])[18] was observed. Rather, substrate- (or possibly product-) bound ferric DHP B(Y28F/Y38F) [401 (Soret), 508, 540 (sh) nm] was the first spectrum recorded, and a conversion to oxyferrous DHP B(Y28F/Y38F) [415 (Soret), 542, 578 nm] was noted after 697 or 120 s for reactions performed with 10 or 50 equiv 5-Br-indole, respectively.

The main observations from these studies employing ferric DHP B were (i) both Compound ES and Compound I were rapidly reduced by 5-Br-indole to the ferric enzyme, and (ii) ferric DHP was further reduced to oxyferrous DHP. Reduction of ferric DHP to the oxyferrous form has been previously observed with dichloroquinone,[13,14,17] the product of trichlorophenol oxidative dehalogenation by DHP, which suggested that a reaction product related to the 5-Br-indole reactivity described above may have led to a similar product-driven reduction chemistry being observed.

Stopped-Flow Studies with Oxyferrous DHP B. As previously reported, oxyferrous DHP is only activated toward reactivity with H_2O_2 (forming Compound II)[17] in the presence of 1 equiv TCP substrate.[17,22] In the absence of substrate, a slight bleaching of the Soret band and/or long time scale conversion to Compound RH have been noted, but no fast time scale reactive intermediates were observed. Such substrate-dependent activation of DHP was investigated here with indole substrates using stopped-flow methods. Upon rapid mixing of a
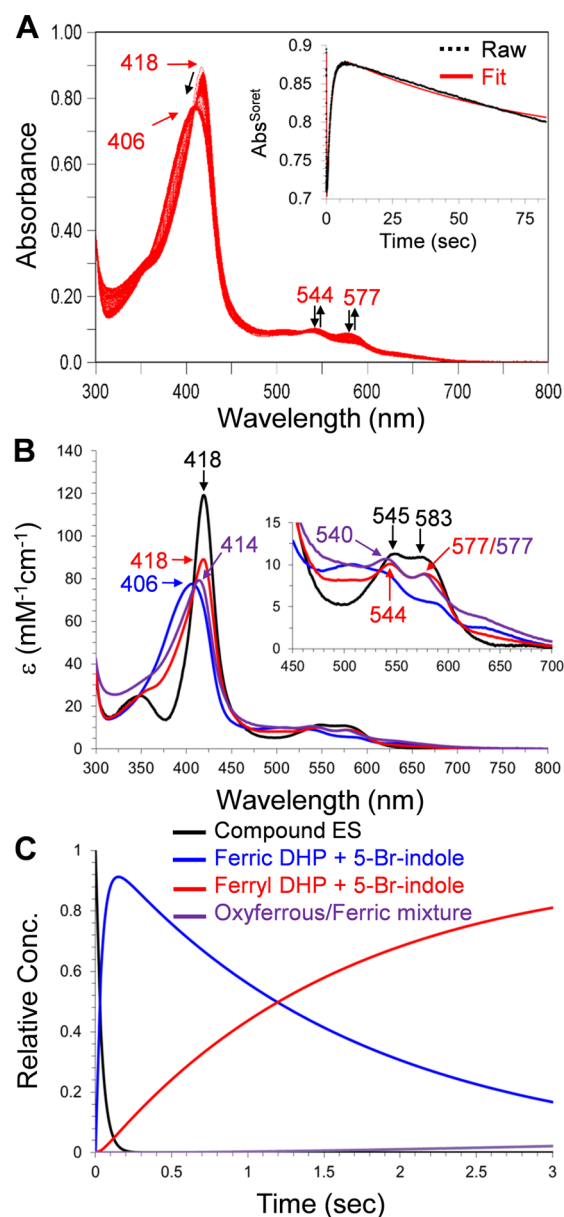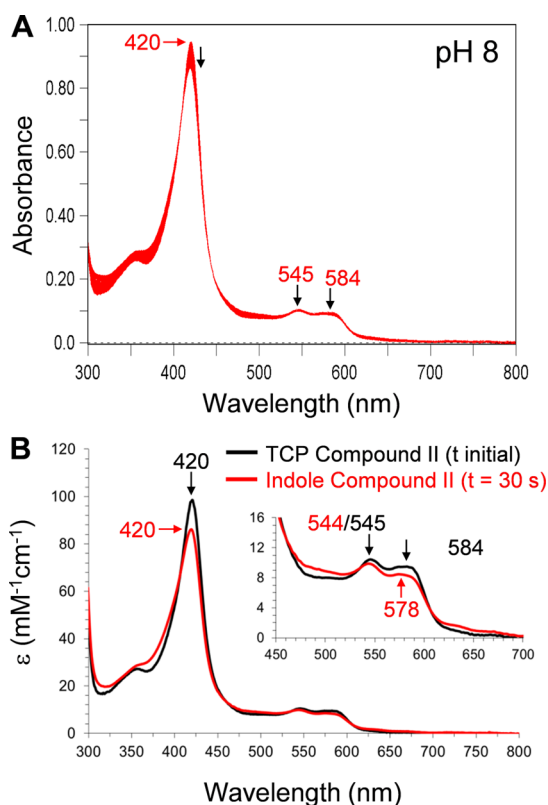

Figure 5. Kinetic data obtained by optical spectroscopy for the reaction of preformed Compound ES with 5-Br-indole. (A) Stopped-flow UV−vis spectra of the double-mixing reaction of preformed DHP B Compound ES (10 μM), itself formed in an initial mixing step from ferric DHP reacted with a 10-fold excess of H_2O_2 in an aging line for 350 ms, with a 10-fold excess of 5-Br-indole at pH 7.0 (800 scans over 83 s). Inset: The single wavelength (418 nm) dependence on time obtained from the raw spectra and its fit with a superposition of the calculated spectral components. (B) Calculated spectra of the four reaction components derived from the SVD analysis: Compound ES (black), ferric DHP B in the presence of excess 5-Br-indole (blue), ferryl DHP in the presence of 5-Br-indole (red), and a mixture of oxyferrous and ferric DHP B (purple). (C) Time dependences of the relative concentrations for the four components shown in the middle panel as determined from the fitting of the spectra in the top panel.

solution of oxyferrous DHP B preincubated with 2.5 equiv of 5-Br-indole with 5 equiv of H_2O_2, substantial spectral changes were observed (Figure 6). The oxyferrous form converted to a species whose spectral features [420 (Soret), 544, 584 nm; $k_{obs} = (3.30 \pm 0.01) \times 10^{-2}$ s^{-1}] matched those of Compound II formed from our previous identification of this species when

7918

dx.doi.org/10.1021/ja500293c | J. Am. Chem. Soc. 2014, 136, 7914−7925
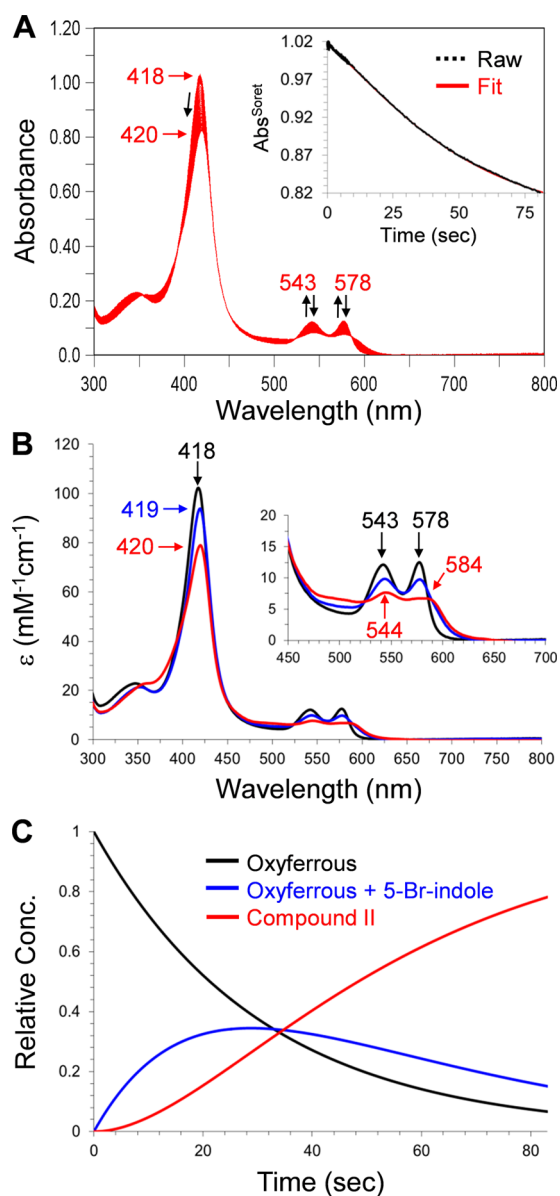
Figure 6. Kinetic data obtained by optical spectroscopy for the reaction of oxyferrous DHP B with 5-Br-indole and hydrogen peroxide. (A) Stopped-flow UV−vis spectra of the single-mixing reaction between oxyferrous DHP B (10 μM) preincubated with 2.5 equiv 5-Br-indole and a 5-fold excess of H_2O_2 at pH 7.0 (800 scans over 83 s). Inset: The single wavelength (418 nm) dependence on time obtained from the raw spectra and its fit with a superposition of the calculated spectral components. (B) Calculated spectra of the three reaction components derived from the SVD analysis: oxyferrous DHP B (black), a mixture of oxyferrous DHP with 5-Br-indole (blue), and DHP B Compound II (red). (C) Time dependences of the relative concentrations for the three components shown in the middle panel as determined from the fitting of the spectra in the top panel.

employing TCP as the substrate.[17] However, when higher equivalents of indole were employed, the intermediate observed had spectral features that were similar [420 (Soret), 545, 578, 584 (sh) nm] (data not shown; *vide infra*), but not identical, to authentic TCP-derived Compound II. We surmise that the presence of the indole in the active site led to these minor spectral differences. The indole-derived Compound II species was found to convert at longer times to the ferric enzyme.


Figure 7. Kinetic data obtained by optical spectroscopy for the reaction of preformed DHP B Compound II with 5-Br-indole. (A) Stopped-flow UV−vis spectra of the double-mixing reaction between preformed DHP B Compound II (10 μM) and 25 equiv 5-Br-indole at pH 8.0 (800 scans over 83 s). DHP B Compound II was itself formed from an initial reaction between oxyferrous DHP B preincubated with 1 equiv trichlorophenol and 10 equiv H_2O_2 and reacted for 85 s prior to the second mix with 5-Br-indole. (B) Experimentally obtained spectra for Compound II derived from TCP (black, $t = 2.5$ ms), and Compound II observed in the presence of 5-Br-indole ($t = 30$ s).

Overall, 5-Br-indole was found to activate oxyferrous DHP toward reactivity with H_2O_2 via a Compound II intermediate.

To further investigate the reactivity of DHP B Compound II, sequential double-mixing stopped-flow studies were employed to monitor the reaction of preformed Compound II with 5-Br-indole substrate. Oxyferrous DHP B containing 1 equiv TCP was reacted with 10 mol equiv of H_2O_2 at pH 8, incubated for 85 s to allow for the maximum accumulation of Compound II [420 (Soret), 545, 584 nm],[17] and subsequently mixed with an additional 10 equiv (Figure S7) or 25 equiv (Figure 7) of 5-Br-indole. Conversion of the Compound II spectrum from the one in the absence of indole to the one observed in the presence of indole [420 (Soret), 545, 578, 584 (sh) nm] was noted in all cases. The disappearance of indole-derived Compound II and the formation of the ferric enzyme were linearly dependent on the concentration of 5-Br-indole cosubstrate, yielding a bimolecular rate constant of $(8.15 \pm 0.26) \times 10^2$ M^{-1} s^{-1}. At concentrations of 5-Br-indole above 25 equiv, the ferric form of the enzyme was further found to partially convert to oxyferrous DHP (data not shown) as noted above for other experiments with this substrate.

Reactivity Studies of 5-Br-3-oxindole. The primary products of 5-Br-indole reactivity, identified to be 5-bromo-2-oxindole and 5-bromo-3-oxindolenine (*vide supra*), were investigated as the putative reductants that led to the observed
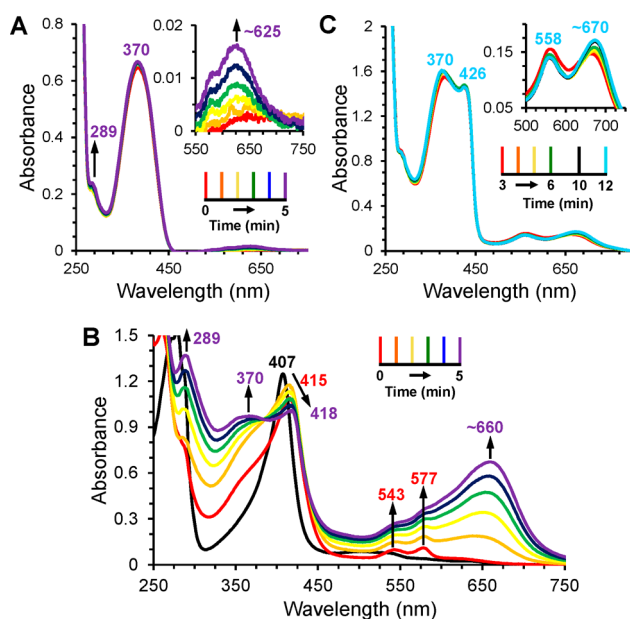
Figure 8. (A) UV−vis spectra obtained under anaerobic conditions of 5-Br-3-oxindole after addition of liver esterase to a solution of 5-Br-3-acetoxyindole (∼250 μM) in 5% MeOH in 100 mM KP$_i$ (pH 7) scanned at times indicated (aerobic). Inset: Spectral region showing minimal 5,5′-Br$_2$-indigo formation. (B) UV−vis spectra obtained under aerobic conditions of 5-Br-3-acetoxyindole (∼250 μM) and ferric DHP B (10 μM) in 5% MeOH in 100 mM KP$_i$ (pH 7) prior to (black spectrum) and 0−5 min after the addition of liver esterase. (C) UV−vis spectra obtained under anaerobic conditions of 5-Br-3-oxindole (∼250 μM) and ferric DHP B (10 μM) from 3 to 12 min after the addition of liver esterase. Inset: Spectral region showing 5,5′-Br$_2$-indigo formation.

formation of oxyferrous DHP in the above stopped-flow studies. 5-Br-2-oxindole, unreactive in the HPLC studies above as a substrate, was unable to reduce ferric DHP B even at 100 equiv (data not shown). Thus, our attention focused on 5-bromo-3-oxindole, the precursor of 5-bromo-3-oxindolenine, as a potential reductant.

In the absence of DHP, UV−vis spectroscopic monitoring of a 250 μM solution of 5-Br-3-oxindole (λ_{max} = 383 nm), formed *in situ* from the hydrolysis of 5-bromo-3-acetoxyindole by porcine liver esterase (LE, 45 U), under aerobic conditions showed only a trace of 5,5′-Br$_2$-indigo formation (λ_{max} = 289 and 640 nm; Figure 8A) after 5 min, likely attributable to the known (non-enzymatic) oxidation of 3-oxindole and derivatives by O$_2$.[43] In the presence of DHP, however, the first spectrum obtained after addition of LE (∼3 s) showed new features [415 (Soret), 543, 577 nm] that closely resembled those of oxyferrous DHP B with a minor component of ferric enzyme present, indicative of DHP reduction by 5-Br-3-oxindole and subsequent binding of O$_2$ under aerobic conditions (Figure 8B). New spectral features at 289, 370, and 659 nm, corresponding to the formation of 5,5′-Br$_2$-indigo, were also noted. Full formation of oxyferrous DHP B [418 (Soret), 543, 577 nm] was seen after 2 min, however the reaction proceeded to generate 5,5′-Br$_2$-indigo throughout the entire 5 min observation period. Using the molar absorptivity coefficient of indigo (22 140 M^{-1} cm^{-1})[44] for 5,5′-Br$_2$-indigo, we estimate the latter's concentration after 5 min to be ∼31 μM, or 45-fold greater, when formed in the presence of DHP versus the absence of enzyme. As a control, the absorption spectrum of 10

μM ferric DHP [407 (Soret), 508 nm] incubated with 250 μM 5-Br-3-acetoxyindole (λ_{max} = 280 nm) exhibited no spectral changes (data not shown).

When the above enzymatic reaction was repeated under anaerobic conditions, the first spectrum obtained after addition of LE in a glovebox and subsequent removal to the spectrophotometer (∼3 min) in a sealed cuvette showed new features [426 (Soret), 558 nm] that closely matched those of ferrous DHP B,[17] suggesting reduction of the ferric enzyme by 5-Br-3-oxindole (Figure 8C). 5,5′-Br$_2$-indigo formation (λ_{max} = 659 nm) was also observed. No other significant changes in the spectral features were observed at longer times. The concentration of 5,5′-Br$_2$-indigo was estimated to be ∼8 μM, or nearly stoichiometric with respect to the enzyme concentration, under anaerobic conditions after 10 min. Overall, nearly 4-fold greater 5,5′-Br$_2$-indigo formation was observed under aerobic (31 μM) versus anaerobic (8 μM) conditions when DHP was present, both of which were higher than the non-enzymatic aerobic control (0.7 μM).

O$_2$-Consumption Studies. The reaction of 5-Br-3-oxindole (500 μM), formed *in situ* from the hydrolysis of 5-bromo-3-acetoxyindole by liver esterase (LE, 45 U), with ferric WT DHP B (10 μM) at pH 7 was monitored for O$_2$-consumption using a dissolved oxygen probe. Prior to the addition of LE, the oxygen concentration was determined to be 17.49 ± 0.20 mg/L (547 ± 6 μM) at room temperature. After 5 min from the addition of LE, the [O$_2$] was 10.12 ± 0.84 mg/L (316 ± 26 μM) yielding a Δ[O$_2$] of 7.37 ± 0.86 mg/L. The non-enzymatic control exhibited Δ[O$_2$] of 1.71 ± 0.51 mg/L after 5 min.

Stopped-Flow Studies with 5-Br-3-oxindole. Single-mixing stopped-flow UV−vis spectroscopic methods were used to investigate the reaction of 25 equiv 5-Br-3-oxindole with 10 μM ferric WT DHP B (Figure 9). Upon their rapid mixing, oxyferrous DHP B [417 (Soret), 543, 578 nm] formation was observed after 8 s, in line with the reactivity studies of 5-Br-3-oxindole described above. At longer observation times, the features related to oxyferrous DHP remained, whereas a new, broad feature ∼600 nm, suggestive of 5,5′-Br$_2$-indigo, was also observed to form. When repeated with oxyferrous DHP B (Figure S8), the spectral features of the enzyme were unchanged as oxyferrous and 5,5′-Br$_2$-indigo formed at the same rate (k_{obs} = 0.021 ± 0.001 s^{-1}) as was previously observed when starting with the ferric enzyme. These results suggested that the reactivity with 5-Br-3-oxindole yielding 5,5′-Br$_2$-indigo could be initiated from either the ferric or oxyferrous states. Under these conditions, no Compound RH was observed.

Double-mixing stopped-flow methods were also used to investigate the reaction of 5-Br-3-oxindole with preformed Compound ES (Figure S9). Ferric WT DHP B (10 μM) was reacted with 5 mol equiv of H$_2$O$_2$ at pH 7, incubated for 350 ms to allow for the maximum accumulation of Compound ES,[14] and subsequently mixed with 25 equiv of 5-Br-3-oxindole. After 8 s, Compound ES [UV−vis: 417 (Soret), 545, 590 nm] was converted to a species whose spectral features we attribute to oxyferrous DHP B [417 (Soret), 543, 578 nm]. At longer observation times, the spectral features of oxyferrous DHP persisted, while significant 5,5′-Br$_2$-indigo formation was also noted after 83 s. No Compound RH was observed.

■ DISCUSSION

The activity studies presented herein demonstrated that dehaloperoxidase was able to catalyze the conversion of
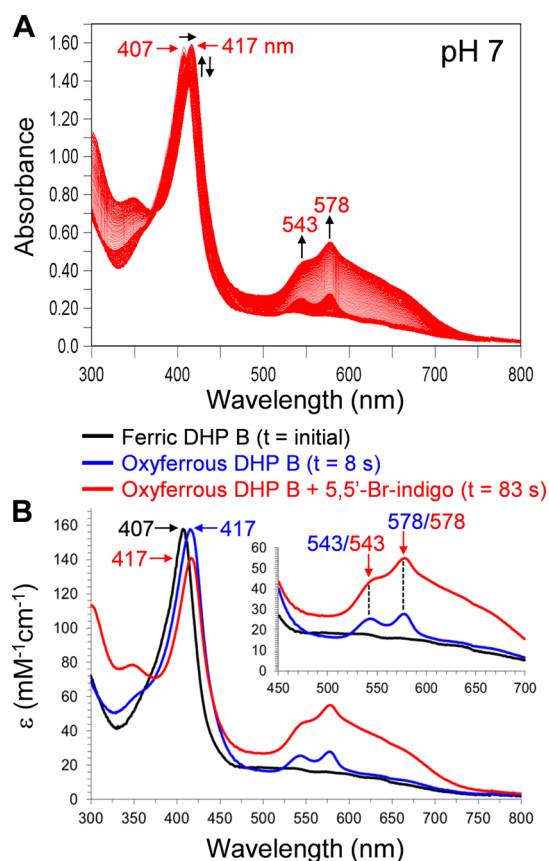
Figure 9. Kinetic data obtained by optical spectroscopy for the reaction of ferric DHP B with 5-Br-3-oxindole. (A) Stopped-flow UV−vis spectra of the double-mixing reaction of ferric DHP B (10 μM) with a 25-fold excess of 5-Br-3-oxindole at pH 7.0 (800 scans over 83 s). 5-Br-3-oxindole was itself formed from an initial reaction between 5-Br-3-acetoxyindole and liver esterase in an aging line prior to the second mix with ferric DHP B. (B) Experimentally obtained spectra for ferric DHP B (black, t = 2.5 ms), oxyferrous DHP B (blue, t = 8 s), and a mixture of oxyferrous DHP B and 5,5′-Br$_2$-indigo (red, t = 83 s).

haloindoles, a previously unreported class of substrate for DHP that is likely physiologically relevant given their production by infaunal organisms that coinhabit the benthic ecosystems within which *A. ornata* resides.[28,29] Activity was observed for all monohaloindoles studied, regardless of the type of halogen or its position on the six-membered ring; however, tryptophan itself was not found to be a substrate. Isotope labeling studies showed that the oxygen atom incorporated into the major (monooxygenated) products was derived exclusively from hydrogen peroxide, analogous to the "peroxide-shunt" of cytochrome P450s and indoleamine 2,3-dioxygenase.[2,34−36] In line with a peroxygenase mechanism, substrate reactivity readily proceeded under anaerobic conditions as well as in the presence of superoxide dismutase and radical quenchers. Such peroxygenase chemistry had been previously unreported for dehaloperoxidase with any substrate.

Activation of most ferric heme proteins by H_2O_2 generally leads to Compound I formation, the Fe(IV)-oxo porphyrin π-cation radical species that is two electrons oxidized compared to the resting enzyme and has been implicated as the principal reactive species in peroxidases,[45] P450s,[34,35] and other hemoproteins.[46,47] By contrast, ferric WT DHP forms Compound ES, a species that like Compound I is also two-electrons oxidized above resting, yet whose second oxidizing

equivalent resides on an amino acid (tyrosyl radical) rather than on the porphyrin ring.[13,14,18] Our results show that DHP Compound I and Compound ES are both capable of reacting with haloindoles, with both being rapidly reduced back to the ferric state (<200 ms for Compound ES, <2.5 ms for Compound I). By comparison, the reaction of preformed WT DHP Compound ES with TCP substrate under similar conditions also reforms the ferric enzyme but is ~10^2-10^4-fold slower (18.5 s).[13,14]

While no mechanistic insight was derived from the stopped-flow studies for the reduction of the ferryl species given the apparent time scale of these reactions, a secondary reaction was noted. Namely, the reduction of the ferric enzyme and formation of oxyferrous DHP were observed. Two lines of evidence suggested a product-driven reduction of ferric DHP: first, we have previously observed for ferric DHP that its reaction with H_2O_2 and TCP ultimately regenerates the oxyferrous enzyme and that separately the product of that reaction, dichloroquinone, is capable of reducing ferric DHP to the oxyferrous state.[13,14,17] While the details of that reaction remain poorly understood, we proposed that the unusually high redox potential of DHP (206 ± 6 mV)[14,16] helped facilitate the reduction of the enzyme by the reaction products after the initial peroxidase activity was completed.[8] Second, Mauk and co-workers recently described the reduction of ferric IDO to ferrous IDO by 3-oxindole that was itself generated as a product during the oxidation of indole by ferric IDO and H_2O_2.[36] It was these two precedents of product-driven reduction of a heme protein that provided the motivation to explore if 5-Br-3-oxindole was able to reduce ferric DHP, which was, in fact, observed to be the case.

On the basis of the results obtained above, and through modification of the previously established mechanisms for peroxygenases,[2,34−36] we propose the following catalytic cycle for the *in vitro* hydrogen peroxide-dependent oxidation of haloindoles by ferric DHP from *A. ornata* (Scheme 1): ferric DHP reacts with 1 equiv H_2O_2, forming either Compound I (step i) or Compound ES (step iii). The reaction of either of these two ferryl species with haloindole leads to the regeneration of the ferric enzyme (steps ii and iv for Compounds I and ES, respectively), with incorporation of the oxygen atom into indole yielding either 5-Br-2-oxindole or 5-Br-3-oxindole. The latter subsequently reacts with the ferric enzyme, leading to oxyferrous DHP formation (v) and the observed 5-Br-3-oxindolenine product. The initial step of substrate reactivity can likely be viewed as hydrogen atom abstraction to yield an indolyl substrate radical[48,49] and an Fe(IV)−OH that subsequently undergoes oxygen rebound to generate indoxyl/oxindole; however, we cannot rule out other possible mechanisms for oxygen atom insertion into an arene,[50] including indole epoxidation via an electrophilic ferryl species.

Alternatively, we have previously proposed that, although counter to monofunctional peroxidase conventions, a bifunctional peroxidase-hemoglobin such as DHP may be able to initiate a peroxidase catalytic cycle from the globin-active oxferrous, and not ferric, state.[8] Oxyferrous DHP reacts with 1 equiv H_2O_2 in the presence of haloindole substrate forming Compound II (step vi), analogous to this substrate-dependent activation that has been observed previously with TCP.[17] At this point, two possibilities must be considered. The first is that oxindole formation occurs upon transfer of the oxygen atom from Compound II, regenerating ferrous DHP which can rebind O_2 under aerobic conditions (not shown). In this

Scheme 1. Proposed Peroxygenase Cycle for Ferric and Oxyferrous Dehaloperoxidase B
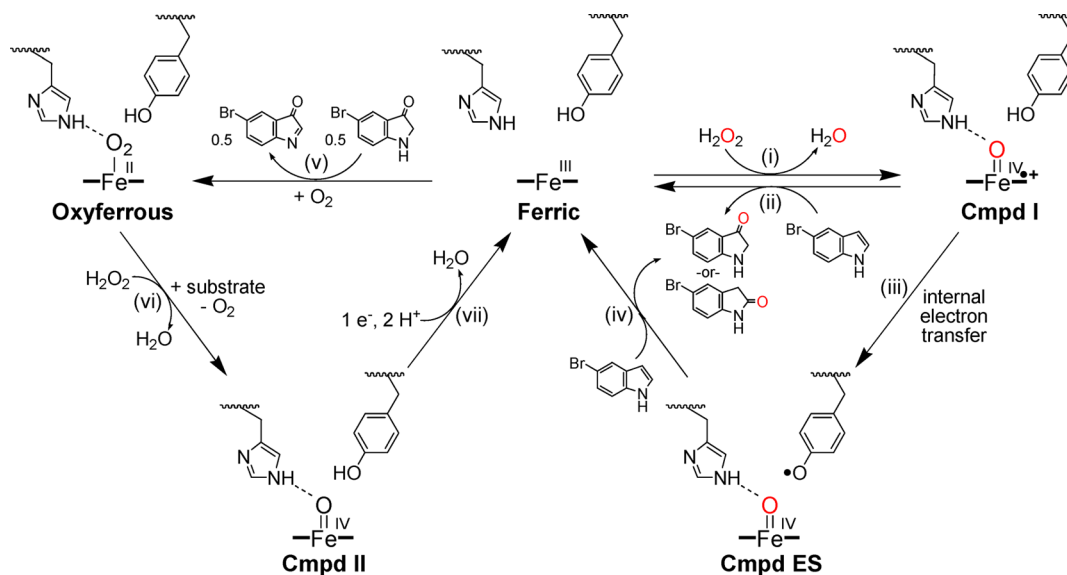
pathway, the two-electron chemistry (Fe^{2+}/Compound II) is occurring in a similar fashion as in the pathway initiated from the ferric state (Fe^{3+}/Compound I or ES). Our results, however, suggest that this pathway does not occur as Compound II reduction clearly yielded the ferric enzyme. The second possibility is that an initial one-electron process occurs where the enzyme is reduced from Compound II to the ferric state by haloindole (step vii) and that the subsequent reactivity proceeds as described above for a typical peroxidase. Overall, however, it is clear that peroxygenase chemistry can be initiated from the globin-active oxyferrous state and that the 3-oxindole reactivity leads back to this state as well.

The oxygen atom transfer chemistry strongly suggests that the haloindole substrate must be in close proximity to the active ferryl intermediate to form the observed products. The results of the haloindole resonance Raman study can be interpreted in light of the two known halophenol binding sites. The addition of 5-X-indole (X = I, Br, Cl) to DHP led to an observed increase in the 5cHS heme population. This is reminiscent of monohalophenol binding, which has been shown to bind in the distal pocket above the heme, and forces the distal histidine to a solvent exposed conformation.[10,37,41,51,52] This ultimately leads to the loss of the iron-bound water ligand and an increase in the 5cHS heme population. We suggest a similar binding location for the 5-haloindoles, as denoted in Figure 4B. By contrast, none of the other bromoindoles (4-, 6-, or 7-) led to changes in the resonance Raman spectrum. We interpret this result to suggest that these substrates bind elsewhere in the distal cavity, possibly in the recently identified tribromophenol binding site that is located in the pocket above the α-edge of the heme (Figure 4C).[40,53] Tribromophenol binding to DHP also does not perturb the resonance Raman spectrum of the ferric enzyme.[14] Given that two binding sites may be present, structural studies may play an important role in deducing whether concerted or nonconcerted (radical) mechanisms form the basis for the observed peroxygenase activity in DHP.

Indole oxidation chemistry has been reported previously: HRP is reactive toward both indole and derivatives (including 5-Br-3-indole acetic acid) via a peroxidase mechanism,[49,54] and a recent report has shown that engineered myoglobin is able to catalyze the oxidation of indole to form indigo blue.[55] Under

the conditions examined here, however, neither of these native monofunctional archetypes of the peroxidase and globin families, respectively, were reactive toward 5-Br-indole, a result that highlights the unique reactivity of the dehaloperoxidase-hemoglobin system. Indoleamine 2,3-dioxygenase has also been shown to catalyze the oxidation of indole via a peroxygenase mechanism, however the product distribution is different.[36] Notably, the major products of indole oxidation with IDO are 2- and 3-oxindole in a ~3:1 ratio when [indole] > [H_2O_2], vs an ~1:1 ratio of 2-oxindole and 3-oxindolenine for DHP. We surmise that the peroxidase activity of DHP led to the oxidation of 3-oxindole to yield the observed 3-oxindolenine product. Further, unlike IDO that was found to be reactive with both 2- and 3-oxindole, DHP exhibited no reactivity toward 5-Br-2-oxindole, a result that suggests that the minor dioxygented products observed must be derived exclusively from the 5-Br-3-oxindole pathway, and likely in a similar fashion that has been reported for P450s.[50,56] Other minor differences between these two enzymes in the product distribution of the dioxygenated products are also evident, but the secondary reactions that led to them in DHP were not further explored.

The investigation of 5-Br-3-oxindole as the reducing agent that led to oxyferrous DHP formation also revealed an unexpected activity for DHP: not only did the aerobic reaction of ferric DHP with 5-Br-3-oxindole (*in situ* generated) immediately form oxyferrous DHP but also gave 5,5′-Br_2-indigo in an amount that exceeded the predicted reaction stoichiometry. Under anaerobic conditions, the yield of 5,5′-Br_2-indigo was near stoichiometric with respect to the enzyme concentration, showing that excess O_2 was obligatory for the catalytic generation of the indigo species by DHP. The non-enzymatic, aerobic oxidation of 5-Br-3-oxindole only produced a trace of 5,5′-Br_2-indigo over the same time scale, showing that DHP was also obligatory for the catalytic generation of the indigo species. Moreover, O_2 consumption studies showed a significant decrease in dissolved oxygen concentration beyond that exhibited by the background (non-enzymatic) reaction, providing confirmatory evidence that the reaction was indeed consuming molecular oxygen. Taken together, the requirements for both dioxygen and DHP in the catalytic formation of 5,5′-Br_2-indigo from the respective oxindole demonstrated an

apparent oxidase activity of dehaloperoxidase-hemoglobin. As to the mechanism of the oxidase activity, based upon these initial observations we propose that, in analogy with the cytochrome P450 catalytic cycle, the one-electron reduction of oxyferrous DHP by 5-Br-3-oxindole yields a ferric-peroxo (Compound 0) intermediate that undergoes O−O bond cleavage to yield Compound ES. The reaction of Compound ES with 5-Br-3-oxindole, as supported by the stopped-flow UV−vis spectroscopic studies, leads to the formation of oxyferrous DHP, likely through a ferric intermediate that is reduced (as above) to the ferrous enzyme and subsequently binds dioxygen, thereby enabling the next round of the oxidase catalytic cycle.

◼ CONCLUSION

In summary, DHP has now been shown to possess peroxygenase and oxidase activities in addition to its previously identified O_2-binding and peroxidase functions. What appears to control for each activity is a complex set of parameters that depends, in part, on the nature of the substrate as well as the dual identity of DHP as both an enzyme and a globin: (i) the relatively high redox potential and protein fold of DHP, hallmarks of the globin family that impart reversible O_2-binding, also lead to its ease of reduction by 3-oxindole, thereby leading to DHP oxidase activity; (ii) an active site pocket capable of halophenol and haloindole binding, unnecessary for an O_2 transport globin, supports both peroxidase and peroxygenase activities, respectively; (iii) a highly flexible distal histidine ligand capable of both stabilizing bound O_2 and serving as a general acid/base catalyst; and (iv) a sterically hindered substrate in 2,4,6-tribromophenol is a DHP peroxidase substrate, whereas the unhindered (at the C2 and C3 positions) haloindole is susceptible to DHP peroxygenase activity, possibly due to the ability of the ferryl intermediate to perform an electrophilic attack on the latter. Other factors, such as the reactivity of Compound I vs Compound ES, the redox potential of the substrate or its pK_a, likely are important determinants of enzymatic activity as well.

The diverse range of functions exhibited by DHP highlights the versatility of this heme protein. The trade-off in being a more versatile enzyme is that DHP exhibits catalytic efficiencies below its monofunctional counterparts, albeit far greater than what is noted as side reactivity in other systems. This increased versatility at the expense of high catalytic efficiency is possibly attributable to the nature of the DHP active site in that it lacks the additional structural features normally observed in more specialized systems that tune the protein toward one specific discrete function. Thus, DHP provides a platform for probing in detail how nature evolved structure−function relationships in ancestral multifunctional systems of competent catalytic activity from lower organisms to achieve the complexity necessary for specialization of function and increased activity observed in the monofunctional systems of higher organisms.

◼ EXPERIMENTAL SECTION

Materials and Methods. Isotopically labeled $H_2^{18}O_2$ (90% ^{18}O-enriched) and $H_2^{18}O$ (98% ^{18}O-enriched) were purchased from Icon Isotopes (Summit, NJ). Acetonitrile (MeCN) was HPLC grade and all other chemicals were purchased from VWR, Sigma-Aldrich, or Fisher Scientific and used without further purification. UV−vis spectroscopy was performed on a Cary 50 UV−vis spectrophotometer. Stock solutions (10 mM) of all indoles were prepared in MeOH, stored in the dark at −20 °C until needed, and were periodically screened by

HPLC to ensure that they had not degraded. Aliquots were stored on ice during use. Solutions of H_2O_2 were prepared fresh daily and kept on ice until needed. The concentration was determined by UV−vis (ε_{240} = 46 mM^{-1} cm^{-1}).[57] Ferric and oxyferrous samples of WT DHP B, DHP B (Y28/38F), and WT DHP A were expressed and purified as previously reported.[13,14,18] Enzyme concentration was determined spectrophotometrically using ε_{Soret} = 116,400 mM^{-1} cm^{-1} for all isoenzymes.[14] Lyophilized horseradish peroxidase and horse heart myoglobin were purchased from Sigma-Aldrich and stored at −20 °C until utilized. Anaerobic studies were performed as described above in an MBraun Lab Master 130 nitrogen-filled glovebox using argon degassed solutions of buffer, peroxide, substrate and enzyme.

Enzyme Assay Protocol. Reactions were performed in triplicate at pH 7 in 5% MeOH in 100 mM KP$_i$ at 25 °C. Buffered solutions (total reaction volume 250 μL) of DHP (10 μM final concentration) and (halo)indole (500 μM final concentration) were premixed, and then the reaction was initiated upon addition of H_2O_2 (50, 100, 250, 500, or 1000 μM final concentrations). Experiments were performed in the presence of D-mannitol (500 μM), superoxide dismutase (SOD) (~2 U/μL), and DMSO (10% v/v). For the studies with sodium formate, a buffered solution (100 mM KP$_i$; 500 mM sodium formate) at pH 7 was utilized. After 5 min, reactions were quenched with excess catalase. A 100 μL aliquot of reaction sample was diluted 10-fold with 900 μL of 100 mM KP$_i$ (pH 7). Diluted samples were analyzed using a Waters 2796 Bioseparations Module coupled with a Waters 2996 Photodiode Array Detector and equipped with a Thermo-Scientific ODS Hypersil (150 mm × 4.6 mm) 5 μm particle size C$_{18}$ column. Separation of observed analytes was performed using a linear gradient of binary solvents (solvent A, H_2O containing 1% trifluoroacetic acid; solvent B, MeCN). Elution was performed using the following conditions: (1.5 mL/min A:B) 95:5 to 5:95 linearly over 10 min; 5:95 isocratic for 2 min; 5:95 to 95:5 linearly over 1 min, and then isocratic for 4 min. Data analysis was performed using the Empower software package (Waters Corp.). Calibration curves for all indoles, and available products were performed using serial dilutions of commercially available analytes to determine the amount of substrate conversion.

LC-MS Studies. Experiments were analyzed using a 6210 LC-TOF mass spectrometer (Agilent Technologies, Santa Clara, CA). Analyte separation was performed using the same conditions and column as the HPLC studies with the exception of solvent A (water with 0.1% formic acid). Samples were analyzed using electrospray ionization in positive ion mode to provide observation of the [M + H]$^+$ species. Spectra were collected each second while scanning in the range from 100−1000 m/z. Data analysis was performed using Agilent software. Quantitation of the amount of ^{18}O-labeled incorporated was performed using previously established methods.[36,38] In the $H_2^{18}O_2$ studies, an aliquot of 2.15% (w/w) solution of 90% enriched $H_2^{18}O_2$ was diluted 3-fold to provide a peroxide solution at 20 mM concentration. A final reaction volume (5% MeOH in 100 mM KP$_i$, pH 7) of 250 μL containing 10 μM enzyme, 50 equiv of substrate, and 50 equiv of labeled peroxide was allowed to react for 5 min before quenching with catalase. For the $H_2^{18}O$ studies, stock solutions of the reactants ([enzyme] = 120 μM; [H_2O_2] = 12.5 mM) in unlabeled water were kept at sufficiently high concentrations to allow for the 98% enriched $H_2^{18}O$ to be diluted to ~89% in the final reaction mixture. Labeled water (207.5 μL) was charged with 21 μL enzyme, 10 μL H_2O_2, and 12.5 μL substrate (in MeOH) and reacted for 5 min and then quenched with catalase. A 20 μL aliquot of undiluted reaction mixtures was injected for LC-MS analysis.

Stopped-Flow UV−vis Studies. Optical spectra were recorded using a Bio-Logic SFM-400 triple-mixing stopped flow instrument coupled to a rapid scanning diode array UV−vis spectrophotometer. The temperature was maintained at 20 °C with a circulating water bath, and all solutions were prepared in 5% MeOH in 100 mM KP$_i$ (variable pH). Data were collected (900 scans total) over a three-time domain regime (2.5, 25, and 250 ms; 300 scans each) using the Bio Kinet32 software package (Bio-Logic). All data were evaluated using the Specfit Global Analysis System software package (Spectrum Software Associates) and fit to exponential functions as one-step/two-

species, two-step/three species or three-step/four species irreversible mechanisms where applicable. For data that did not properly fit these models, experimentally obtained spectra at selected time points shown in the figure legends are shown. Data were baseline corrected using the Specfit autozero function.

Experiments were performed in single-mixing mode where enzyme at a final concentration of 10 μM was reacted with 2.5−25 equiv of H_2O_2. For substrate preincubation studies, the enzyme solution also contained substrate (2.5−50 equiv). Double mixing experiments were performed using an aging line prior to the second mixing step to observe Compound ES/Compound I reactivity with 5- or 7-Br-indole substrate (2.5−50 equiv). For studies with 5-Br-3-oxindole, a solution of 5-Br-3-acetoxyindole in 100 mM potassium phosphate buffer was prepared from a 10 mM stock solution in pure methanol for final concentrations of 100, 250, or 500 μM. The 5-Br-3-acetoxyindole solutions were loaded into the stopped-flow syringe, and ∼1 mg (20 U) of liver esterase was directly added to the syringe and mixed thoroughly, and then the solution was loaded into the apparatus. Control experiments were also performed as above in the absence of hydrogen peroxide.

Resonance Raman Studies. Samples were prepared with final concentrations of 50 μM WT DHP B and 500 μM substrate in 100 mM KP$_i$ (pH 7) containing 10% MeOH (v/v) and then transferred to a 5 mm diameter glass NMR tube. Spectra were obtained by Soret band excitation using a Coherent Mira 900 titanium sapphire (Ti:sapphire) laser. The Ti:sapphire laser was pumped using a Coherent Verdi 10 frequency doubled diode pumped Nd:vanadate (Nd:VO$_4$) laser producing 10 W at 532 nm. The beam generated was sent through a Coherent 5-050 doubler to generate a normal working range of 400−430 nm for Soret band excitation of both DHP only and the DHP/indole complexes. The beam was collimated and cylindrically focused to a vertical line of ∼0.5 mm on the sample. Laser power at the sample was 60 mW. Scattered light was collected with a Spex 1877 triple spectrometer equipped with a liquid nitrogen-cooled CCD detector controlled by Spectramax software.

Geometry Optimization Studies. The native substrate 2,4,6-tribromophenol (2,4,6-TBP) in the structure PDB 4HF6[40] was substituted with 7-bromoindole. Since diatomic O_2 was observed bound to the heme Fe in that structure, the bound O_2 was preserved in this model. The 5-bromoindole model was obtained by replacement of 4-bromophenol in the PDB 3LB2 structure.[37] In this model, the bromine atom is located in the Xe binding site[39] as observed in the 4-bromophenol structure. The parameters for the 5-bromo and 7-bromoindole molecules were obtained by modification of the tyrosine amino acid from the CHARMM force field implemented in the NAMD code[58,59] with a charge set calculated using electrostatic potential fitting[60] implemented in the density functional theory (DFT) code DMol3.[61,62] The DFT calculations were conducted using a double numerical basis set with polarization functions and the PBE functional.[63,64] The charge set and templates for the NAMD topology file are provided in the Supporting Information. The bond stretching, bending, and torsional parameters for the C−Br bond and associated angles and dihedrals were obtained from the structure and an estimate of the relative bond stretching force constant. Visual molecular dynamics (VMD) was used for visualization and generation of the figures.[65]

Haloindole-Binding Studies. Adapted from previously published protocols,[42] stock solutions of 2 mM 5-X-indole (X = F, Cl, Br and I) in MeOH were prepared. The UV−vis spectrophotometer was blanked with 10 μM ferric WT DHP B in 100 mM KP$_i$ (pH 7) containing 10% MeOH. Spectra were then acquired in the presence of 2.5, 5, 10, 25, 50, and 100 equiv of the indole substrates while maintaining both constant enzyme and MeOH concentrations. Analysis by nonlinear regression using the GraFit software package (Erithacus Software Ltd.) of the experiments performed in triplicate provided a calculated A_{max}, which was in turn used to calculate α for the average ΔA for each indole concentration. A nonlinear regression plot provided the reported apparent K_d values.

Studies with 5-Br-3-oxindole. 250 μM 5-Br-3-acetoxyindole was incubated in the presence or absence of 10 μM ferric WT DHP B in

5% MeOH in 100 mM KP$_i$ at pH 7 (<1 min) in a quartz cuvette. Reactions were initiated by the addition of porcine liver esterase (LE, 45 U), and spectra collected at the times indicated. Anaerobic studies were initiated in the glovebox, the quartz cuvette was sealed from the atmosphere, and the spectra were obtained on the benchtop.

O$_2$-Consumption Studies. All experiments were performed in triplicate with a Fisher Scientific AR 60 dissolved oxygen Accumet BOD probe that was standardized in dH$_2$O prior to use. Solutions of 5-Br-3-acetoxyindole in methanol were freshly prepared prior to each experiment. Ten mg of liver esterase was dissolved in 500 mL of 100 mM KP$_i$ buffer and kept on ice. A 5 mL solution was made containing 10 μM ferric WT DHP B and 500 μM 5-Br-3-acetoxyindole in 5% MeOH in 100 mM KP$_i$ buffer (pH 7), and the meter was stabilized in the solution. A 50 μL aliquot of porcine liver esterase (∼1 U/μL) was added to the 5 mL solution, and the final O$_2$ concentration was measured after 6 min.

ASSOCIATED CONTENT

Ⓢ Supporting Information

UV−vis spectra of **1a−1f** and **2a−2f**, reactivity studies of DHP with indole and product distribution tables, resonance Raman spectra of indole and 4-, 5-, 6-, and 7-Br-indole with DHP B, optical difference spectra and titration curves of 5-X-indole binding to DHP B, additional kinetic data and stopped-flow studies of DHP B with 5-Br-indole and 5-Br-3-oxindole, mass spectrometric analyses of isotope labeling studies, and the charge set and templates for the NAMD topology file. This material is available free of charge via the Internet at http://pubs.acs.org.

AUTHOR INFORMATION

Corresponding Author
Reza_Ghiladi@NCSU.edu
Notes
The authors declare no competing financial interest.

ACKNOWLEDGMENTS

REFERENCES

(1) Yoshikawa, S.; Muramoto, K.; Shinzawa-Itoh, K. *Annu. Rev. Biophys.* **2011**, *40*, 205.

(2) Denisov, I. G.; Makris, T. M.; Sligar, S. G.; Schlichting, I. *Chem. Rev.* **2005**, *105*, 2253.

(3) Lu, C.; Yeh, S. R. *J. Biol. Chem.* **2011**, *286*, 21220.

(4) Wang, X.; Peter, S.; Kinne, M.; Hofrichter, M.; Groves, J. T. *J. Am. Chem. Soc.* **2012**, *134*, 12897.

(5) Dunford, H. B.; Stillman, J. S. *Coord. Chem. Rev.* **1976**, *19*, 187.

(6) Poulos, T. L. *Chem. Rev.* **2014**.

(7) Egawa, T.; Shimada, H.; Ishimura, Y. *J. Biol. Chem.* **2000**, *275*, 34858.

(8) Franzen, S.; Thompson, M. K.; Ghiladi, R. A. *Biochim. Biophys. Acta* **2012**, *1824*, 578.

(9) Weber, R. E.; Mangum, C.; Steinman, H.; Bonaventura, C.; Sullivan, B.; Bonaventura, J. *Comp. Biochem. Physiol., Part A: Comp. Physiol.* **1977**, *56*, 179.

(10) Lebioda, L.; LaCount, M. W.; Zhang, E.; Chen, Y. P.; Han, K.; Whitton, M. M.; Lincoln, D. E.; Woodin, S. A. *Nature* **1999**, *401*, 445.

(11) Zhang, E.; Chen, Y. P.; Roach, M. P.; Lincoln, D. E.; Lovell, C. R.; Woodin, S. A.; Dawson, J. H.; Lebioda, L. *Acta Crystallogr., Sect. D: Biol. Crystallogr.* **1996**, *52*, 1191.

(12) Osborne, R. L.; Taylor, L. O.; Han, K. P.; Ely, B.; Dawson, J. H. *Biochem. Biophys. Res. Commun.* **2004**, *324*, 1194.

(13) Feducia, J.; Dumarieh, R.; Gilvey, L. B.; Smirnova, T.; Franzen, S.; Ghiladi, R. A. *Biochemistry* **2009**, *48*, 995.

(14) D'Antonio, J.; D'Antonio, E. L.; Thompson, M. K.; Bowden, E. F.; Franzen, S.; Smirnova, T.; Ghiladi, R. A. *Biochemistry* **2010**, *49*, 6600.

(15) Thompson, M. K.; Franzen, S.; Ghiladi, R. A.; Reeder, B. J.; Svistunenko, D. A. *J. Am. Chem. Soc.* **2010**, *132*, 17501.

(16) D'Antonio, E. L.; D'Antonio, J.; de Serrano, V.; Gracz, H.; Thompson, M. K.; Ghiladi, R. A.; Bowden, E. F.; Franzen, S. *Biochemistry* **2011**, *50*, 9664.

(17) D'Antonio, J.; Ghiladi, R. A. *Biochemistry* **2011**, *50*, 5999.

(18) Dumarieh, R.; D'Antonio, J.; Deliz-Liang, A.; Smirnova, T.; Svistunenko, D. A.; Ghiladi, R. A. *J. Biol. Chem.* **2013**, *288*, 33470.

(19) Osborne, R. L.; Sumithran, S.; Coggins, M. K.; Chen, Y. P.; Lincoln, D. E.; Dawson, J. H. *J. Inorg. Biochem.* **2006**, *100*, 1100.

(20) Osborne, R. L.; Coggins, M. K.; Raner, G. M.; Walla, M.; Dawson, J. H. *Biochemistry* **2009**, *48*, 4231.

(21) Davydov, R.; Osborne, R. L.; Shanmugam, M.; Du, J.; Dawson, J. H.; Hoffman, B. M. *J. Am. Chem. Soc.* **2010**, *132*, 14995.

(22) Du, J.; Sono, M.; Dawson, J. H. *Biochemistry* **2010**, *49*, 6064.

(23) de Serrano, V.; D'Antonio, J.; Franzen, S.; Ghiladi, R. A. *Acta Crystallogr., Sect. D: Biol. Crystallogr.* **2010**, *66*, 529.

(24) Poulos, T. L.; Kraut, J. *J. Biol. Chem.* **1980**, *255*, 8199.

(25) Woodin, S. A.; Walla, M. D.; Lincoln, D. E. *J. Exp. Mar. Biol. Ecol.* **1987**, *107*, 209.

(26) Woodin, S. A. *Am. Zool.* **1991**, *31*, 797.

(27) Chen, Y. P.; Woodin, S. A.; Lincoln, D. E.; Lovell, C. R. *J. Biol. Chem.* **1996**, *271*, 4609.

(28) Gribble, G. W. *Chem. Soc. Rev.* **1999**, *28*, 335.

(29) Gribble, G. W. *Environ. Sci. Pollut. Res. Int.* **2000**, *7*, 37.

(30) Bansal, T.; Englert, D.; Lee, J.; Hegde, M.; Wood, T. K.; Jayaraman, A. *Infect. Immun.* **2007**, *75*, 4597.

(31) Lee, J. T.; Jayaraman, A.; Wood, T. K. *BMC Microbiol.* **2007**, *7*, 42.

(32) Valeriote, F. A.; Tenney, K.; Media, J.; Pietraszkiewicz, H.; Edelstein, M.; Johnson, T. A.; Amagata, T.; Crews, P. *J. Exp. Ther. Oncol.* **2012**, *10*, 119.

(33) Bharate, S. B.; Manda, S.; Mupparapu, N.; Battini, N.; Vishwakarma, R. A. *Mini. Rev. Med. Chem.* **2012**, *12*, 650.

(34) Sono, M.; Roach, M. P.; Coulter, E. D.; Dawson, J. H. *Chem. Rev.* **1996**, *96*, 2841.

(35) Meunier, B.; de Visser, S. P.; Shaik, S. *Chem. Rev.* **2004**, *104*, 3947.

(36) Kuo, H. H.; Mauk, A. G. *Proc. Natl. Acad. Sci. U. S. A.* **2012**, *109*, 13966.

(37) Thompson, M. K.; Davis, M. F.; de Serrano, V.; Nicoletti, F. P.; Howes, B. D.; Smulevich, G.; Franzen, S. *Biophys. J.* **2010**, *99*, 1586.

(38) Mirgorodskaya, O. A.; Kozmin, Y. P.; Titov, M. I.; Korner, R.; Sonksen, C. P.; Roepstorff, P. *Rapid Commun. Mass Spectrom.* **2000**, *14*, 1226.

(39) de Serrano, V.; Franzen, S. *Biopolymers* **2012**, *98*, 27.

(40) Zhao, J.; de Serrano, V.; Le, P.; Franzen, S. *Biochemistry* **2013**, *52*, 2427.

(41) Nicoletti, F. P.; Thompson, M. K.; Howes, B. D.; Franzen, S.; Smulevich, G. *Biochemistry* **2010**, *49*, 1903.

(42) Chenprakhon, P.; Sucharitakul, J.; Panijpan, B.; Chaiyen, P. *J. Chem. Educ.* **2010**, *87*, 829.

(43) Joule, J. A.; Mills, K. *Heterocyclic chemistry*; 5th ed.; Wiley: Hoboken, NJ, 2009.

(44) de Melo, J. S.; Moura, A. P.; Melo, M. J. *J. Phys. Chem. A* **2004**, *108*, 6975.

(45) Dunford, H. B. *Heme Peroxidases*; Wiley-VCH: New York, 1999.

(46) Matsui, T.; Ozaki, S.; Liong, E.; Phillips, G. N., Jr.; Watanabe, Y. *J. Biol. Chem.* **1999**, *274*, 2838.

(47) Matsui, T.; Ozaki, S.; Watanabe, Y. *J. Biol. Chem.* **1997**, *272*, 32735.

(48) de Melo, M. P.; Escobar, J. A.; Metodiewa, D.; Dunford, H. B.; Cilento, G. *Arch. Biochem. Biophys.* **1992**, *296*, 34.

(49) Ximenes, V. F.; Campa, A.; Catalani, L. H. *Arch. Biochem. Biophys.* **2001**, *387*, 173.

(50) Guengerich, F. P. *Chem. Res. Toxicol.* **2001**, *14*, 611.

(51) Davis, M. F.; Gracz, H.; Vendeix, F. A.; de Serrano, V.; Somasundaram, A.; Decatur, S. M.; Franzen, S. *Biochemistry* **2009**, *48*, 2164.

(52) de Serrano, V. S.; Davis, M. F.; Gaff, J. F.; Zhang, Q.; Chen, Z.; D'Antonio, E. L.; Bowden, E. F.; Rose, R.; Franzen, S. *Acta Crystallogr., Sect. D: Biol. Crystallogr.* **2010**, *66*, 770.

(53) Wang, C.; Lovelace, L. L.; Sun, S.; Dawson, J. H.; Lebioda, L. *Biochemistry* **2013**, *52*, 6203.

(54) Jantschko, W.; Furtmuller, P. G.; Allegra, M.; Livrea, M. A.; Jakopitsch, C.; Regelsberger, G.; Obinger, C. *Arch. Biochem. Biophys.* **2002**, *398*, 12.

(55) Xu, J. K.; Shoji, O.; Fujishiro, T.; Ohki, T.; Ueno, T.; Watanabe, Y. *Catal. Sci. Technol.* **2012**, *2*, 739.

(56) Gillam, E. M.; Notley, L. M.; Cai, H.; De Voss, J. J.; Guengerich, F. P. *Biochemistry* **2000**, *39*, 13817.

(57) Beers, R. F., Jr.; Sizer, I. W. *J. Biol. Chem.* **1952**, *195*, 133.

(58) Phillips, J. C.; Braun, R.; Wang, W.; Gumbart, J.; Tajkhorshid, E.; Villa, E.; Chipot, C.; Skeel, R. D.; Kale, L.; Schulten, K. *J. Comput. Chem.* **2005**, *26*, 1781.

(59) Nelson, M.; Humphrey, W.; Gursoy, A.; Dalke, A.; Kale, L.; Skeel, R. D.; Shulten, K. *Int. J. Supercomput. Appl. High Perform. Comput.* **1996**, *10*, 251.

(60) Ferenczy, G. G. *J. Comput. Chem.* **1991**, *12*, 913.

(61) Delley, B. *J. Chem. Phys.* **1990**, *92*, 508.

(62) Delley, B. *J. Chem. Phys.* **2000**, *113*, 7756.

(63) Perdew, J. P.; Burke, K.; Wang, Y. *Phys. Rev. B: Condens. Matter* **1996**, *54*, 16533.

(64) Perdew, J. P.; Wang, Y. *Phys. Rev. B: Condens. Matter* **1992**, *45*, 13244.

(65) Humphrey, W.; Dalke, A.; Schulten, K. *J. Mol. Graphics* **1996**, *14*, 33.